

# **Characteristics of one year of observational data of VOCs, NO<sub>x</sub> and O<sub>3</sub> at a suburban site in Guangzhou, China**

**Y. Zou<sup>1,2</sup>, X. J. Deng<sup>1,2</sup>, B. G. Wang<sup>2</sup>, F. Li<sup>1</sup>, H. B. Tan<sup>1</sup>, T. Deng<sup>1</sup>, B. R. Mai<sup>1</sup>, and X. T. Liu<sup>1</sup>**

<sup>1</sup>Institute of Tropical and Marine Meteorology/Guangdong Provincial Key Laboratory of Regional Numerical Weather Prediction, CMA, Guangzhou, China

<sup>2</sup>Institute of Atmospheric Environmental Safety and Pollution Control, Jinan University, Guangzhou, China

Received: 3 June 2014 – Accepted: 21 June 2014 – Published:

Correspondence to: X. J. Deng (dxj@grmc.gov.cn) and B. G. Wang (tbongue@jnu.edu.cn)

Published by Copernicus Publications on behalf of the European Geosciences Union.

## Abstract

In this study, online monitoring instruments were used to monitor ozone, NO<sub>x</sub> and VOCs from the Guangzhou Panyu Atmospheric Composition Station (GPACS) of the China Meteorological Administration from June 2011 to May 2012, so as to obtain their characteristics and relationships of VOCs, NO<sub>x</sub> and ozone. The results show that during the observation period, the seasonal variation of ozone concentration was lower in spring and winter, while being higher in summer and autumn, which is contrary to that of the VOCs and NO<sub>x</sub>. Aromatics are the largest components for ozone formation potential, among which toluene, m-xylene, p-xylene and 1,3,5-trimethylbenzene are the most important components, with a total contribution of about 31.6% to ozone formation potential. The peak ozone during high-concentration ozone events is likely to be NO<sub>x</sub>-limited as indicated by analyzing the relationship among VOCs, NO<sub>x</sub> and the amount of ozone increase ( $\Delta O_3$ ), and further confirmed by measured VOCs/NO<sub>x</sub> ratio, which suggests that peak ozone production is more likely to be sensitive to changes in NO<sub>x</sub> during summer and autumn, and thus presenting a reference for ozone control in Guangzhou.

## 1 Introduction

Along with its rapid economic development and urbanization, the Pearl River Delta has become one of the most serious pollution areas in China (Chan et al., 2008). Different from the air pollution situations of Beijing, Tianjin, Hebei and the Yangtze River Delta region, which involve particulate matters as the main pollutants (Wang et al., 2012; Zhao et al., 2011), due to its unique geographical location and climate, as well as the rapid increase in the emissions of ozone precursors (VOCs and NO<sub>x</sub>) caused by industrial activities and the growing number of motor vehicles, high-concentration ozone events occur frequently and have become very prominent air pollution problems in the Pearl River Delta (Wang et al., 2009). Tropospheric ozone is the secondary pollutant generated by photochemical reactions of VOCs and NO<sub>x</sub> under light conditions (Sillman, 1995). However, VOCs and NO<sub>x</sub> have no linear relationship with ozone formation, and their impacts on ozone formation can be described by VOC and NO<sub>x</sub> limited regime (Zhang et al., 2004; Tie et al., 2007; Geng et al., 2008). A large amount of research has been conducted regarding ozone formation in the Pearl River Delta (Wang et al., 2005; Cheng et al., 2010; Guo et al., 2009). Many laboratory studies using some chambers have served to clarify the gas-phase photochemical transformations of NO<sub>x</sub> and VOCs, and their roles in the formation of ozone. The maximum ozone concentrations generated from various mixtures of NO<sub>x</sub> and VOCs are often presented on ozone isopleth diagrams. The numerical simulations showed that although the specific actual situations differ, it is generally considered that when the VOC/NO<sub>x</sub> ratio is more than 8:1, ozone formation regime is NO<sub>x</sub> limited regime, while the VOC/NO<sub>x</sub> ratio is less than 8:1, ozone formation regime is VOC-limited (Seinfeld, 1989), which many researchers used to elucidate the characteristics of photochemical ozone production (Sillman, 1999; Committee on Tropospheric Ozone Formation and Measurement, 1991; Ran et al., 2009, 2011). However, little attention has been given to the VOC/NO<sub>x</sub> ratio and the relationship among VOCs, NO<sub>x</sub> and  $\Delta O_3$  using observational data. In addition, most previous studies performed in the Pearl River Delta region reported that ozone is VOC-limited (Zhang et al., 2008b; Guo et al., 2009). However, few previous studies on the region's ozone formation regime have examined the possible diurnal variations in ozone formation regime.

Currently, a greater amount of systematic long-term observation data on atmospheric ozone and NO<sub>x</sub> has become available, while VOCs data which mostly involves short-term intensive observations or non-continuous long term observations is not included in the scope of daily observations (Wang et al., 2004; Shao et al., 2009). Therefore, the relationship among VOCs, NO<sub>x</sub> and ozone can't be fully revealed to discern the impacts of VOCs and NO<sub>x</sub> on ozone formation in the Pearl River Delta region. In order to more effectively solve the problem of ozone pollution in the Pearl River Delta, VOCs, NO<sub>x</sub> and ozone were observed throughout the period of one year at GPACS, focusing on analyzing the characteristics of VOCs, NO<sub>x</sub> and ozone, as well as VOCs components in ozone formation. In addition, the relationship among VOCs, NO<sub>x</sub> and  $\Delta O_3$  using observational data is plotted to elucidate the characteristics of photochemical ozone productions. Finally, the VOC/NO<sub>x</sub> ratio by observational data was also used to analyze the ozone formation regime with diurnal variation in Guangzhou, which has only been done by a small number of scholars (Li et al., 2008). In order to reveal the occurrence of high-concentration ozone events in Guangzhou, ozone formation regimes with

diurnal variation are explored in four scenarios herein, i.e. spring, summer, autumn and winter.

This study is organized as follows. The second section describes the methodology used in this study, also including the sampling point and observation instruments. The third section  
5 mainly analyzes the observed results, including characteristic analyses of ozone, NO<sub>x</sub> and VOCs, as well as an analysis of the contribution of VOCs components to ozone formation by using MIR and an equivalent propylene concentration method. In the final section, the relationship among VOCs, NO<sub>x</sub> and  $\Delta O_3$  by observational data is plotted to elucidate the characteristic of photochemical ozone production, and the VOC/NO<sub>x</sub> ratio analysis method is  
10 also adopted to analyze ozone formation in the seasonal diurnal variation process.

## 2 Methodology

### 2.1 Measurements

15 From June 2011 to May 2012, automatic sampling and on-line monitoring were carried out on ozone, NO<sub>x</sub> and VOCs. The sampling site was located at the mountain top of Dazhengang, Nancun Town, Panyu District, Guangzhou City, Guangdong Province, China with an elevation of 141 m, at the latitude of 23° 00.236' N and longitude of 113° 21.292' E (Fig. 1).  
20 This sampling station is located in suburban Guangzhou in which the high ozone events often occur, and is the main site of the observation network for atmospheric composition in Pearl River Delta. Fig.2 shows that regardless of the large variation in concentration of the three types of VOCs, the relative contribution of the three groups remains fairly uniform throughout the observational time. Such uniformity implies that air was sufficiently homogenized from  
25 various sources at the surface. The prevailing wind, wind speed and temperature at the sampling point during the different seasons are shown in Fig. 3 and Table 1. At the sampling point, northeasterly and southwesterly are the prevailing winds in spring (April, May and June), along with southwesterly in summer (June, July and August), southwesterly in autumn (September, October and November), and northeasterly in winter (December, January and  
30 February). In the different seasons, the average wind speed varies at around 1.4ms<sup>-1</sup>, while the average temperature undergoes more significant changes from 14.2°C in winter to 29.4°C in summer. Typical air pollution processes can also be seen in different seasons and under different weather conditions. When the prevailing wind is northeasterly in December, the difference between weekends and weekdays for VOCs is very typical, showing large amounts  
35 of pollutants are emitted from downtown Guangzhou City. When the prevailing wind is southwesterly in July, the difference between weekends and weekdays for VOCs is not apparent, for the reason that only small amounts of pollutants are emitted from the further suburban areas (Fig.1).

### 40 2.2 Instrument description

The data used in this study include the hourly concentration of ozone, NO<sub>x</sub> and VOCs during the observation period (June 2011–May 2012). The concentration of ozone gas was obtained using an EC9810B ozone analyzer produced by Ecotech Co. of Australia with the UV

photometric method. It's measured in a single glass measuring tank and calculated by Lambert-Beer Law. The concentration of nitrogen oxides gas was collected using an EC9841B oxynitride (NO/NO<sub>2</sub>/NO<sub>x</sub>) gas analyzer produced by Ecotech with the chemiluminescence method. The instrument has a single channel. Sample gas will bypass and go through a molybdenum converter respectively. NO is measured by chemiluminescence in a reaction cell, NO<sub>2</sub> is converted to NO by using a molybdenum converter. After that, NO value and NO<sub>x</sub> value will be collected and the difference is NO<sub>2</sub> value. The NO<sub>x</sub> may include some oxidized reactive nitrogen that is converted by the molybdenum, and thus that the stated mixing ratios in result and discussion are upper limits to the actual NO<sub>x</sub>. VOCs concentration was obtained using a GC5000 analyzer produced by AMA Co. of Germany with the GC-FID analysis method. This latter apparatus is comprised of a low boiling- point VOC analyzer and high-boiling-point BTX analyzer, including two sets of sampling systems and two systems of separated chromatographic columns. A low boiling- point VOC analyzer was able to conduct enriched concentration on a tube which is filled with special adsorption materials at 13°C, a second adsorption at 20°C, and desorption when the temperature was raised to 200°C, followed by separation with two-dimensional chromatographic columns. The chromatographic columns consisted of a Al<sub>2</sub>O<sub>3</sub>/Na<sub>2</sub>SO<sub>4</sub> plot column with a diameter of 0.32 mm, film thickness of 5mm and length of 60 m, as well as a back flushing column (carbowax) with a diameter of 0.32 mm, film thickness of 0.25mm and length of 30 m. A back flushing column was used to remove the moisture component and high boiling component, and two types of chromatographic column were polar columns. Through two rounds of thermal desorption, the low-boiling-point hydrocarbons could be well separated, and the detector was a flame ionization detector (FID). A BTX high-boiling-point analyzer was able to conduct precondensation of volatile organic compounds at 30°C, followed by thermal desorption, then separation on the DB-1 column to achieve optimum separation and prevent interference of related compounds. This column has a diameter of 0.32 mm, thickness of 10mm and length of 60 m. A flame ionization detector (FID) was used to detect the system. The detected target compounds were 56 kinds of VOCs designated by the US EPA with the time resolution of once per hour, and the standards we used were the same as those used by the EPA/USA PAMs (Photochemical Assessment Monitoring Stations), The analytical method was described in a previous study (Zou et al., 2013). The QA/QC of online VOC measurements was performed. Before and after the observation period, we performed a zero gas check for memory effect or contamination and a span gas check with PAMs calibration gas in order to check the drift, repeatability and memory effects. We normally got standard curve which qualified the species by using a five point calibration method and retention time which quantified the species. The standard curve and the detection line of VOCs are listed in Table 2. You can see that correlation coefficient ranged from 0.984 to 0.999, and detection limit ranged from 0.03ppbv to 0.09ppbv. During the observation period, we also performed a span gas check every month by using one point calibration and adjust the retention time. Finally, outliers need to be eliminated to guarantee the valid data.

### **3 Results and discussion**

#### **3.1 Characteristics of ozone, NO<sub>x</sub> and VOCs**

The seasonal diurnal variation characteristics of ozone, VOCs and NO<sub>x</sub> are shown in Fig. 4. The seasonal variation characteristic of ozone is relatively apparent, which displays the seasonal pattern of being lower in the spring and winter and higher in the summer and autumn. Furthermore, the increase range is much larger in late spring and early summer than the other periods, which is mainly due to the light, temperature, other meteorological factors and emissions strength of air pollutants being different in each season (Bloomer et al., 2009, 2010). The seasonal variation in the concentration of ozone precursors is opposite to that of ozone concentration. NO<sub>x</sub> concentration is higher in spring and winter, but lower in summer and autumn and VOCs concentration is higher in winter, but lower in summer. Average concentration of VOCs, NO<sub>x</sub> and ozone in four seasons are showed in table 3. VOCs concentration varies from 34.60ppbv in March to 63.57ppbv in November, NO<sub>x</sub> concentration varies from 21.75ppbv in August to 76.39 in March, and ozone concentration varies from 9.31ppbv in January to 29.67 in September. The diurnal concentration variation of ozone is unimodal, reaching its maximum at 2.00 p.m., while those of the ozone precursors, i.e. VOCs and NO<sub>x</sub>, show a bimodal variation with a peak in rush hours, though variations may be not apparent among some seasons. These diurnal concentration variations exhibit the characteristic that photochemical precursors gradually reduce and products increase accordingly. It should be noted that mixing ratios in this are upper limits to the actual NO<sub>x</sub> because of that NO<sub>x</sub> may include some oxidized reactive nitrogen that is converted by the molybdenum. In order to further understand the variation in ozone concentration and reveal its dependence on photochemical reactions, it is necessary to analyze the derivatives with respect to time of ozone in four seasons, shown as follows:

$$d[O_3]/dt = [O_3](t + 1h) - [O_3](t) \quad (1)$$

In the equation, [O<sub>3</sub>](*t*) represents the ozone concentration at time *t*, and [O<sub>3</sub>](*t* + 1 h) is the ozone concentration for the next hour of time *t*. A negative derivative variation in ozone concentration indicates that the chemical loss of ozone plays a dominant role in the variation in ozone concentration, while the contrary indicates the fact that the generation of ozone photochemical reactions plays a key role. Horizontal transport effect is very small due to the fact that wind speed varies at around 1.4ms<sup>-1</sup> in different seasons (table 1). Though the diurnal variations in the ozone derivative in different seasons display a little difference, the results show that a negative derivative of variation in ozone concentration occurs at about 15:00LT, the OH radicals become lower and titration of ozone by emissions of NO<sub>x</sub> plays a key role. At about 19:00LT, there is no OH radicals and NO titration could still consume ozone, until the NO titration ceased, the ozone concentration remained a relatively stable during the period (0:00-7:00LT). The concentration trend of ozone begins to show a positive derivative variation at 8:00LT due to the breakup of the nocturnal boundary layer, high OH radicals and a strong photochemical reaction when the sun rise (Fig. 5).

### 3.2 The effect of each VOCs category on ozone formation

VOCs appear in various kinds, and their concentrations do not correspond to their ozone formation. Different kinds of VOCs have different photochemical reactivities, thereby leading to different ozone formation potential. Controlling the species with the largest ozone

formation potential is the most cost-effective solution to ozone control. VOCs have two main factors for ozone formation potential: kinetic activity and mechanism activity. For kinetic activity, the propylene-equivalent concentration method ( $C_{PE}(J)$ ) is expressed as shown below:

$$C_{PE}(J) = C_J K_{OH}(J) / K_{OH}(C_3H_6) \quad (2)$$

In the equation, J represents a species of VOC,  $C_J$  represents the carbon-number concentration (ppbc) of this species, and  $K_{OH}(J)$  and  $K_{OH}(C_3H_6)$  denote the chemical reaction rate constant in the free radical reaction of species J and propylene with OH.  $K_{OH}(J)$  is obtained from Atkinson and Aery (Atkinson and Aery, 2003). The reaction rate constant is shown in Table 4. For the

mechanism activity, the MIR factor weighting method is used with the following expression:

$$Con_{j,MIR} = MIR \times Com_{ppbv} \times u_j / u_{ozone} \quad (3)$$

In the equation,  $u_{ozone}$  represents the molecular mass of ozone, and  $u_j$  represents the relative molecular mass of species J in the VOCs,  $Com_{ppbv}$  represents the actual volume mixing ratio, the Maximum Incremental Reactivity (MIR) factors were developed by Carter in model Scenarios, the MIR of each VOCs is looked up from his reference (Carter et al., 1994), and  $Con_{j,MIR}$  is maximum-increment-activity MIR factor weighting concentration which represents the maximum ozone concentration generated by this species based on MIR. The maximum ozone concentrations of different VOCs are used to compare their relative ozone formation potential. The MIR coefficients are shown in Table 4.

Fig.6 shows the characteristics of each VOCs category obtained at the sampling point by using the volume mixing ratio concentration (ppbv), carbon number concentration (ppbc), propylene-equivalent concentration (ppbc), and maximum-increment-activity MIR factor weighting concentration (ppbv) methods. As viewed from the volume mixing ratio concentration (ppbv) and carbon number concentration (ppbc), alkanes occupy the largest proportion, accounting for 59% and 53% of the total VOCs concentration respectively; followed by aromatics (24% and 36% respectively), and alkenes have the lowest proportion, at 17% and 11% respectively. As viewed from propylene-equivalent and MIR factor weighting concentrations, the alkenes and aromatics are dominant, accounting for total proportions of 73% and 83% respectively, and alkanes have the lowest proportion. Total propylene-equivalent concentration accounts for nearly half of the total carbon concentration, indicating that the activities of major VOCs species are lower than propylene at the sampling point. In summary, during the monitoring period, as viewed from the volume mixing ratio and carbon number concentrations of VOCs, alkanes and aromatics are shown to be the highest mixing ratio of the atmosphere at the sampling point. However, as viewed from ozone formation potential, aromatics and alkenes are the two species with the largest contributions. The alkane content is high, but because of their low reactivity, alkanes have less contribution to the reactivity of VOCs and ozone formation potential. Although the alkenes concentrations are smaller than those of alkanes, due to their high reactivity, alkenes have greater contributions to ozone than alkanes.

Table 5 shows the ozone formation potential ranking of VOCs species as calculated by the propylene-equivalent concentration and MIR factor methods. It can be seen that the results of both methods are partially consistent, but some differences may also be seen. Among the top ten species, eight species are exactly the same, differing only in terms of rank order. It is shown that both methods can be used to reflect the ozone formation potential of each VOCs

species to some extent, and especially those with greater contributions to ozone formation have better consistency. However, since these two methods differ in principle, the calculated ranks of ozone formation potential are also different. The propylene-equivalent concentration method only considering kinetic activity ignores the differences in mechanism activities of the reaction between peroxide radicals and NO, thus when assessing ozone formation potential, the species with faster OH reaction rate may be overestimated, such as isoprene. Although the MIR factor method considers the kinetics and mechanism activity, due to the fact that the MIR factor involves possible uncertainty and the lack of MIR data for some species, the MIR factor method cannot become a reliable assessment approach of ozone formation potential. In addition, it should be noted that MIR determined in one location may be different in another, so that the application of MIR would be approximately correct in Guangzhou. In summary, aromatics are the species with the highest reactivity at the sampling site, followed by alkenes. Toluene, m-xylene, p-xylene and 1,3,5-trimethylbenzene with higher reactivity have a total contribution to ozone formation potential of about 31.61%. These species are mainly sourced from large factories and industrial activities (Liu et al., 2008a). As an industrial city, Dongguan City (circle on the map in Fig.1) is presumed to have some contributions to these species at sampling site in the autumn and winter, due to the fact that it is located in the eastern part of the sampling site and northeasterly wind is the prevailing in the autumn and winter at the sampling site. Moreover, isoprene has no high concentration, but ranks at first and third in terms of OH activity and MIR respectively. Therefore, the isoprene emissions need to be considered with respect to the control of ozone in Guangzhou.

### 3.3 Ozone formation regime

VOCs and NO<sub>x</sub> have a non-linear relationship with the formation of the ozone as a secondary photochemical product, and their impacts on the ozone formation can be described by the VOCs and NO<sub>x</sub> control areas. The peak ozone concentrations generated from various initial concentrations of NO<sub>x</sub> and VOCs were usually presented as an ozone isopleth diagram, in which initial mixture compositions giving rise to the same peak ozone concentrations are connected by the appropriate ozone isopleth diagrams can be generated for different VOCs mixtures and for different levels of solar intensity from modeling studies using the validated chemical mechanisms (Dodge, 1977). To elucidate the photochemical potential to produce ozone in Guangzhou City, observational data selected by meteorological conditions are used to plot the relationship among VOCs, NO<sub>x</sub> and ΔO<sub>3</sub>. Different from the numerical simulations, this included all processes such as transport, deposition and mixing, in addition to chemical reactions that control the ozone concentration. Accordingly, we selected the days when the sum of the hourly solar radiation data from sunrise to 18:00 exceeds the annual average, so as to reduce the influence of irregular solar intensity, and when the average wind speed data from sunrise to 18:00 is < 3ms<sup>-1</sup> so as to reduce the influence of transport. For the NO<sub>x</sub> and VOCs concentrations to generate ozone, the average concentrations of VOCs and NO<sub>x</sub> in the early morning (6:00-9:00) are used, and the amount of ozone increase (ΔO<sub>3</sub>) is defined as the difference between the maximum value in (10:00-18:00) and the average value in the early morning (6:00-9:00) (Fig.7). It shows that when the VOCs concentration is between 0ppbc and 250ppbc, the ozone formation regime is likely to be VOC-limited (i area



in Fig.7), thus reducing the VOCs may reduce ozone formation; when the VOCs concentration is between 250ppbc and 600ppbc, the ozone formation regime is likely to be NO<sub>x</sub>-limited (ii area in Fig.7) and the reduction of NO<sub>x</sub> may reduce ozone formation; and when the VOCs concentration is above 600ppbc, the ozone formation regime is likely to be (VOCs and NO<sub>x</sub>)-limited(iii area in Fig.7), and reducing the VOCs and NO<sub>x</sub> together may reduce the ozone formation. The high  $\Delta O_3$  usually occurs in NO<sub>x</sub>-limited regime which indicated that NO<sub>x</sub> must be controlled to regulate the occurrence of high-concentration ozone events. Ozone formation regime by VOCs concentrations may be decided by the composition of VOCs. Assuming that more active organic carbons are included in the VOCs composition, they are reacted with OH radicals more active than other hydrocarbons and the chain propagating reaction ( $OH+RH\rightarrow R+H_2O$ ) would be more dominant than the chain terminating reaction ( $OH+NO_2(+M)\rightarrow HNO_3(+M)$ ). We select the day(2011.8.12) represented by A point and the day(2011.11.5) represented by B point in Fig.7. Alkanes, alkenes and aromatics are accounting for 50%,18% and 32% of the total VOCs respectively on the day(2011.8.12), while alkanes, alkenes and aromatics are accounting for 58%,17% and 25% of the total VOCs respectively on the day (2011.11.15), more active organic carbons are included in the VOCs composition on the day(2011.8.12). As a result, you can see lower total VOCs concentration on the day(2011.8.12) can produce nearly the same  $\Delta O_3$  as the day(2011.11.5) with higher VOCs concentration, though other factors like meteorology should be taken into account for this. The distribution frequency of hourly ozone concentration in each season could be seen in Fig.8 that higher hourly ozone concentration usually occurs in summer and autumn, the second is spring, but no high hourly ozone concentration occurs in spring. The scatters between VOCs and NO<sub>x</sub> are selected by meteorological conditions in different seasons(Fig.9), most of the scatters under NO<sub>x</sub>-limited(ii area corresponding to Fig.7) and (VOC and NO<sub>x</sub>)-limited (ii area corresponding to Fig.7) correspond to summer and autumn, in which the high ozone episodes usually occur, strengthening the result that when the ozone concentration is very high, the ozone formation regime is likely to be NO<sub>x</sub>-limited. NO<sub>x</sub> control is of importance for peak ozone reduction in Guangzhou City.

In the formation of the tropospheric ozone, the reaction of VOCs and NO<sub>x</sub> with free radicals plays an important role and the ozone formation relies on the VOC/NO<sub>x</sub> ratio. The actual VOC/NO<sub>x</sub> ratio at which ozone production is VOC-limited or NO<sub>x</sub>-limited will depend on specific conditions within a given area, so that the use of a single ratio(8) is only approximate to be referred if detailed photochemical modeling is not available. It's fare to say that the ozone formation is more likely to be NO<sub>x</sub>-limited under the condition that VOC/NO<sub>x</sub> ratio is much higher than value (8); while the ozone formation is more likely to be VOC-limited under the condition that VOC/NO<sub>x</sub> ratio is much lower than value (8). Also, it should be noted that the actual VOC/NO<sub>x</sub> ratio would possibly be larger than shown due to the fact that a molybdenum converter was used for NO<sub>x</sub> measurement as we discussed before. According to these, VOC/NO<sub>x</sub> ratio was used to examine the possible diurnal variations in ozone formation regime, and to give a rough idea about VOC-limited or NO<sub>x</sub>-limited (Fig. 10). In the morning (7:00 to 08:00 LT) in the summer and autumn, the VOC/NO<sub>x</sub> ratio is less than value (8), the ozone formation regime is likely to be VOCs-limited, and a decline in VOCs concentration may help to further reduce the ozone concentration. However, when the ozone concentration reaches a peak at noon, the VOC/NO<sub>x</sub> ratio is much higher than value (8),

and the ozone formation regime is more likely to be NO<sub>x</sub>-limited. The ozone formation regime may shift from VOC-limited in early the morning to NO<sub>x</sub>-limited at noon. Considering the high concentration ozone events are prone to occur in summer and autumn, the NO<sub>x</sub> is more likely to be controlled to achieve the purpose of controlling high-concentration ozone events, which is similar to the research finding in the Pearl River Delta (Li et al., 2013). In the spring and winter, the VOC/NO<sub>x</sub> ratio is always much lower than 8, and ozone formation regime is more likely to be VOC-limited for a long period of time. Since the ozone concentration is relatively low in these two seasons, although the reduction of NO<sub>x</sub> can increase the ozone concentration, no high-concentration ozone event will occur. Therefore, for the control of the local ozone, in addition to VOCs control, the control of NO<sub>x</sub> concentration will further reduce high ozone concentration to prevent the occurrence of high-concentration ozone events, which to some extent prove the point that we showed before. Considering the impact of VOCs to ozone formation is more relevant to the reactivity of individual VOC species rather than to the amount of VOCs, VOC(reactivity)/NO<sub>x</sub> ratio was used to analyze ozone formation(Fig.10).The VOC(reactivity)/NO<sub>x</sub> ratio(PE or MIR) was consistent with the VOC(ppbc)/NO<sub>x</sub> ratio due to the fact that regardless of the large variation in concentration of the three categories of VOCs, the relative contribution of the three groups remains fairly uniform throughout the observation time(Fig.2).

The high-concentration ozone is seriously harmful to human health, many regulators are focusing on reducing emissions at peak ozone forming hours (Castellanos et al., 2009). In order to further study the relationship between actual VOC/NO<sub>x</sub> ratio and ozone formation under the conditions of high-concentration ozone, 36 days with high-concentration ozone were selected for analysis in the monitoring period; the day with high-concentration ozone refers to the day with an hourly ozone value higher than 93 ppbv. You could be seen in Fig.11 that the VOC/NO<sub>x</sub> ratio under the conditions of high-concentration ozone at noon is much higher than in summer and autumn, which indicates that the control of NO<sub>x</sub> is more likely to reduce the peak of high-concentration ozone. However, when the ozone concentration is relatively low in the morning (6:00-9:00) and at night (20:00-0:00), the control of the NO<sub>x</sub> concentration may transiently increase the ozone concentration. Therefore, when high-concentration ozone events occur, more attention need to be paid to controlling NO<sub>x</sub>, so as to achieve the purpose of controlling high-concentration ozone events.

#### 4 Conclusions

One-year (from June 2011 to May 2012) consecutive observation was carried out on the near-surface ozone and its precursors VOCs and NO<sub>x</sub> at GPACS, which is located in suburban Guangzhou where the high ozone events were often occur. Observation-based analysis has been performed to investigate the characteristics of VOCs, NO<sub>x</sub> and ozone in this highly populated region.

The ozone concentration is significantly shown as being lower in the spring and winter and higher in the summer and autumn, while the precursors VOCs and NO<sub>x</sub> display the opposite seasonal variations against the ozone. The concentration trend of ozone begins to show a positive derivative variation at 8:00LT mainly due to the strong photochemical reaction when

the sun rises.

In terms of volume mixing ratio concentration and carbon number of VOCs, alkanes and aromatics are the most important atmospheric categories at the sampling site. As viewed from ozone formation potential, aromatics are the species with the largest contributions. Among these, toluene, m-xylene, p-xylene and 1,3,5-trimethylbenzene are the most important with a total contribution to ozone formation potential of about 31.6%. It should be noted that the concentration of isoprene emitted by plants is not high, but has a very large contribution to the ozone.

The relationship among VOCs, NO<sub>x</sub> and  $\Delta O_3$  by measured data are employed to determine the sensitivity of ozone formation. When the VOCs concentration is between 0ppbc and 250ppbc, the ozone formation regime is likely to be VOC-limited regime; when the VOCs concentration is between 250ppbc and 600ppbc, the ozone formation regime is likely to be NO<sub>x</sub>-limited; and when the VOCs concentration is above 600ppbc, the ozone formation regime is likely to be (VOCs and NO<sub>x</sub>)-limited regime. The high  $\Delta O_3$  is usually occur in NO<sub>x</sub>-limited regime which indicates that NO<sub>x</sub> needs to be controlled to regulate the occurrence of high-concentration ozone events which usually occur in summer and autumn. This phenomenon is further confirmed by measured VOCs/NO<sub>x</sub> ratio, which shows that the ozone formation regime is possibly shift from VOC-limited regime in early the morning to NO<sub>x</sub>-limited regime at noon in summer and autumn, and the NO<sub>x</sub> needs to be controlled to achieve the purpose of controlling high-concentration ozone events. However, in the spring and winter, the ozone formation regime is more likely to be VOC-limited for a long period of time. Since the ozone concentration is relatively low in these two seasons, although the control of the NO<sub>x</sub> can increase the ozone concentration, no high-concentration ozone event will occur.

It should be note that the results are presented above only by observational data, further investigations based on numerical model are needed in the future to obtain more detailed and robust conclusions. Numerical models available nowadays to simulate ozone pollution in the atmosphere like observation-based model (OBM), Weather Research and Forecasting-Chemistry mode (WRF-Chem) and the U.S. Environmental Protection Agency's Community Multi-scale Air Quality (CMAQ) are necessary to describe the formation of ozone from VOCs and NO<sub>x</sub>.

*Acknowledgements* This research work is funded by the National Natural Science Foundation of China (41175117, 40875090), National "973" Program (2011CB403400), Natural Science Foundation of Guangdong Province (S2012010008749), Special Research Project of Public Service Sectors (Weather) (GYHY201306042), and Science and Technology Sponsorship Program of Guangdong Province(2010A030200012)

40

## References

- Atkinson, R. and Arey, J.: Atmospheric degradation of volatile organic compounds, *Chem. Rev.*, 103, 4605–4638, 2003.
- 5 Bloomer, B. J., Stehr, J. W., Piety, C. A., Ross, J. S., and Dickerson, R. R.: Observed relationships of ozone air pollution with temperature and emissions, *Geophys. Res. Lett.*, 36, L09803, doi:10.1029/2009GL037308, 2009.
- Bloomer, B. J., Vinnikov, K. Y., and Dickerson, R. R.: Changes in seasonal and diurnal cycles of ozone and temperature in the eastern US, *Atmos. Environ.*, 44, 1–9, 2010.
- 10 Carter, W. P. L.: Development of ozone reactivity scales for volatile organic compounds, *J. Air Waste Manage.*, 44, 881–899, 1994.
- Castellanos, P., Stehr, J. W., Dickerson R. R., and Ehrman, S. H.: The sensitivity of modeled ozone to the temporal distribution of point, area, and mobile source emissions in the eastern United States, *Atmos. Environ.*, 43, 4603–4611, 2009.
- 15 Chan, C. K. and Yao, X. H.: Air pollution in mega cities in China, *Atmos. Environ.*, 42, 1–42, doi:10.1016/j.atmosenv.2007.09.003, 2008.
- Cheng, H. R., Guo, H., Saunders, S. M., Lam, S. H. M., Jiang, F., Wang, X. M., Simpson, I. J., Blake, D. R., Louie, P. K. K., and Wang T. J.: Assessing photochemical ozone formation in the Pearl River Delta with a photochemical trajectory model, *Atmos. Environ.*, 44, 4199–4208, 2010. Committee on Tropospheric Ozone Formation and Measurement: Rethinking the Ozone Problem in Urban and Regional Air Pollution, Natl. Acad. Press, Washington, DC, 1991.
- 20 Deng, X. J., Wang, X. M., Zhao, C. S., Ran, L., Li, F., Tan, H. B., Deng, T., Wu, D., and Zhou, X. J.: The mean concentration and chemical reactivity of VOCs of typical processes over Pearl River Delta Region, China, *Environ. Sci.*, 30, 1153–1161, 2010.
- Dodge, M. C.: Combined use of modeling techniques and smog chamber data to derive ozone precursor relationship, *Proceedings of the international conference on photochemical oxidant pollution and its control*, 2, 811–899, 1977.
- 25 Geng, F. H., Tie, X. X., Xu, J. M., Zhou, G. Q., Peng, L., Gao, W., Tang, X., and Zhao, C. S.: Characterizations of ozone, NO<sub>x</sub>, and VOCs measured in Shanghai, China, *Atmos. Environ.*, 42, 6873–6883, 2008.
- 30 Guo, H., Jiang, F., Cheng, H. R., Simpson, I. J., Wang, X. M., Ding, A. J., Wang, T. J., Saunders, S. M., Wang, T., Lam, S. H. M., Blake, D. R., Zhang, Y. L., and Xie, M.: Concurrent observations of air pollutants at two sites in the Pearl River Delta and the implication of regional transport, *Atmos. Chem. Phys.*, 9, 7343–7360, doi:10.5194/acp-9-7343-2009, 2009.
- Li, Y.: Numerical Studies on Ozone Source Apportionment and Formation Regime and their Implications on Control Strategies, Hong Kong University of Sci. & Tech., Hong Kong, 2011.
- 35 Li, Y., Lau, K. H., Fung, C. H., Zheng, J. Y., and Liu, S. C.: Importance of NO<sub>x</sub> control for peak ozone reduction in the Pearl River Delta region, *J. Geophys. Res.*, 118, 9428–9443, 2013.
- Liu, Y., Shao, M., Fu, L. L., Lu, S. H., Zeng, L. M., and Tang, D. G.: Source profiles of volatile organic compounds (VOCs) measured in China: part I, *Atmos. Environ.*, 42, 6247–6260, 2008.
- 40 Ran, L., Zhao, C. S., Geng, F. H., Tie, X. X., Xu, T., Li, P., Guang, Q. Z., Qiong, Y., Xu, J. M., and Guenther, A.: Ozone photochemical production in urban Shanghai, China: analysis based on ground level observations, *J. Geophys. Res.*, 114, doi:10.1029/2008JD010752, 2009.
- Ran, L., Zhao, C. S., Xu, W. Y., Lu, X. Q., Han, M., Lin, W. L., Yan, P., Xu, X. B., Deng, Z. Z., Ma, N., Liu, P. F., Yu, J., Liang, W. D., and Chen, L. L.: VOC reactivity and its effect on ozone production during the HaChi

- summer campaign, *Atmos. Chem. Phys.*, 11,4657–4667, doi:10.5194/acp-11-4657-2011, 2011.
- Shao, M., Zhang, Y. H., Zeng, L. M., Tang, X. Y., Zhang, J., Zhong, L. J., and Wang, B. G.: Ground-level ozone in the Pearl River Delta and the roles of VOC and NO<sub>x</sub> in its production, *Environ. Manage.*, 90, 512–518, 2009.
- 5 Sillman, S.: The use of NO<sub>y</sub>, H<sub>2</sub>O<sub>2</sub>, and HNO<sub>3</sub> as indicators for ozone-NO<sub>x</sub>-hydrocarbon sensitivity in urban locations, *J. Geophys. Res.*, 100, 14175–14188, 1995.
- Sillman, S.: The relation between ozone, NO<sub>x</sub> and hydrocarbons in urban and polluted rural environment, *Atmos. Environ.*, 33, 1821–1845, 1999.
- Seinfeld, J.H.. *Urban Air Pollution: State of the Science*, Science, 243, 745-752, 1989.
- Tie, X., Madronich, S., Li, G. H., Ying, Z. M., Zhang, R. Y., Garcia, A. R., Taylor, J. L., and Liu, Y. B.:
- 10 Characterizations of chemical oxidants in Mexico City: a regional chemical/ dynamical model (WRF-Chem) study, *Atmos. Environ.*, 41, 1989–2008, 2007.
- Wang, B. G., Zhang, Y. H., and Shao, M.: Special and temporal distribution character of VOCs in the ambient air of Pearl River Delta region, *Environ. Sci.*, 25, 7–15, 2004.
- Wang, T., Wei, X. L., Ding, A. J., Poon, C. N., Lam, K. S., Li, Y. S., Chan, L. Y., and Anson, M.:
- 15 Increasing surface ozone concentrations in the background atmosphere of Southern China, 1994–2007, *Atmos. Chem. Phys.*, 9, 6217–6227, doi:10.5194/acp-9-6217-2009, 2009.
- Wang, T. J., Jiang, F., Deng, J. J., Shen, Y., Fu, Q. Y., Wang, Q., Fu, Y., Xu, J. H., and Zhang, D. N.: Urban air quality and regional haze weather forecast for Yangtze River Delta region, *Atmos. Environ.*, 58, 70–83, 2012.
- 20 Wang, X. M., Carmichael, G., Chen, D. L., Tang, Y. H., and Wang, T. J.: Impacts of different emission sources on air quality during March 2001 in the Pearl River Delta (PRD) region, *Atmos. Environ.*, 39, 5227–5241, 2005.
- Zhang, R. Y., Lei, W. F., Tie, X. X., and Hess, P.: Industrial emissions cause extreme diurnal urban ozone variability, *P. Natl. Acad. Sci. USA*, 101, 6346–6350, 2004.
- 25 Zhang, Y. H., Su, H., Zhong, L. J., Cheng, Y. F., Zeng, L. M., Wang, X. S., Xiang, Y. R., Wang, J. L., Gao, D. F., and Shao, M.: Regional ozone pollution and observation-based approach for analyzing ozone–precursor relationship during the PRIDE-PRD2004 campaign, *Atmos. Environ.*, 42, 6203–6218, doi:10.1016/j.atmosenv.2008.05.002, 2008.
- Zhao, P. S., Zhang, X. L., Xu, X. F., and Zhao X. J.: Long-term visibility trends and characteristics in the region of Beijing, Tianjin, and Hebei, China, *Atmos. Res.*, 101, 711–718, 2011.
- 30 Zou, Y., Deng, X. J., Wang, B. G., Li, F., and Huang, Q.: Pollution characteristics of volatile organic compounds in Panyu Composition Station, *Environ. Sci.*, 33, 808–813, 2013.

**Table 1.** The wind speed and temperature in four seasons (from June 2011 to May 2012) at GPACS.

		Minimum	Maximum	Mean value	Median
Spring	Windspeed/ms <sup>-1</sup>	0	5.4	1.3	1.2
	Temperature/°C	9.4	35.5	22.6	22.9
Summer	Windspeed/ms <sup>-1</sup>	0	6.0	1.4	1.2
	Temperature/°C	23.9	37.1	29.4	28.8
Autumn	Windspeed/ms <sup>-1</sup>	0	5.7	1.5	1.4
	Temperature/°C	16.2	35.3	25.2	25.2
Winter	Windspeed/ms <sup>-1</sup>	0	6.3	1.5	1.4
	Temperature/°C	4.7	26.9	14.2	14.1

**Table 2.**The standard curve and detection line of VOC species

Target compound	Standard curve	correlation coefficient	Detection limit (ppbv)
Ethylene	$y=1.0188x+0.2659$	0.997	0.07
Acetylene	$y=1.0409x+0.1756$	0.998	0.08
Ethane	$y=1.0162x+0.2891$	0.997	0.08
Propylene	$y=0.9959x+0.1506$	0.999	0.07
Propane	$y=0.9824x+0.2082$	0.998	0.09
Isobutane	$y=0.9753x+0.3785$	0.994	0.05
1-Butene	$y=0.9587x+0.3641$	0.994	0.06
n-Butane	$y=0.9776x+0.3718$	0.994	0.05
t-2-Butene	$y=0.9746x+0.2747$	0.997	0.05
c-2-Butene	$y = 0.9834x+0.1606$	0.999	0.06
Isopentane	$y=0.9753x+0.2135$	0.998	0.07
1-Pentene	$y = 0.919x+0.1626$	0.998	0.05
n-Pentane	$y = 0.9557x+0.2038$	0.984	0.07
Isoprene	$y=1.0304x+0.1653$	0.998	0.07
trans-2-pentene	$y=0.9753x+0.2135$	0.998	0.07
cis-2-pentene	$y = 0.9557x+0.2038$	0.984	0.07
2,2-Dimethylbutane	$y=0.9731x+0.1971$	0.998	0.07
Cyclopentane	$y=0.9993x+0.1412$	0.997	0.06
2,3-Dimethylbutane	$y = 0.919x+0.1626$	0.999	0.07
2-Methylpentane	$y = 0.9557x+0.2038$	0.984	0.07
3-Methylpentane	$y=0.9753x+0.2135$	0.998	0.07
2-Methyl-1-Pentene	$y=0.9700x+0.3300$	0.995	0.05
n-Hexane	$y=0.9915x+0.2626$	0.997	0.06
Methylcyclopentane	$y = 0.9749x+0.1832$	0.999	0.07
2,4-Dimethylpentane	$y=0.9993x+0.1412$	0.999	0.05
Benzene	$y=0.9753x+0.2835$	0.997	0.06
Cyclohexane	$y=0.9841x+0.2744$	0.997	0.07
2-methylhexane	$y=0.9744x+0.2979$	0.996	0.05
2,3-dimethylpentane	$y=0.9779x+0.2953$	0.997	0.05
3-methylhexane	$y=0.9735x+0.3374$	0.995	0.05
2,2,4-trimethylpentane	$y=0.9696x+0.3947$	0.994	0.05
n-Heptane	$y=0.9678x+0.3635$	0.994	0.05
Methylcyclohexane	$y=0.9819x+0.3629$	0.995	0.05
2,3,4-trimethylpentane	$y=0.9691x+0.3994$	0.994	0.04
Toluene	$y=0.9696x+0.3397$	0.995	0.05
2-methylheptane	$y=0.9603x+0.4835$	0.990	0.04
3-methylheptane	$y=0.9625x+0.4550$	0.991	0.04
n-Octane	$y=0.9524x+0.5082$	0.989	0.04
Ethylbenzene	$y=0.9629x+0.4253$	0.992	0.04
m&p-Xylenes	$y=0.9541x+0.5844$	0.986	0.03

---

Styrene	$y=0.9524x+0.4132$	0.991	0.04
o-Xylene	$y=0.9515x+0.4926$	0.989	0.04
n-Nonane	$y = 0.9878x+0.1635$	0.998	0.04
Isopropylbenzene	$y=0.9418x+0.5162$	0.986	0.04
n-Propylbenzene	$y=0.9426x+0.5468$	0.986	0.04
m-Ethyltoluene	$y = 0.9532x+0.4838$	0.989	0.04
p-Ethyltoluene	$y = 0.9554x+0.3953$	0.992	0.04
1,3,5-Trimethylbenzene	$y = 0.951x+0.4724$	0.989	0.04
o-Ethyltoluene	$y = 0.9784x+0.0956$	0.999	0.04
1,2,4-trimethylbenzene	$y = 0.9563x+0.4509$	0.991	0.03
n-Decane	$y = 0.9651x+0.3068$	0.995	0.04
1,2,3-trimethylbenzene	$y = 0.9537x+0.3191$	0.993	0.04
m-Diethylbenzene	$y = 0.9541x+0.4494$	0.991	0.04
p-Diethylbenzene	$y = 0.9607x+0.3788$	0.993	0.04
n-Undecane	$y = 0.9519x+0.3329$	0.992	0.04

---



**Table 3.** Daily average of VOCs and its constituents, NO<sub>x</sub> and ozone in four seasons (from June 2011 to May 2012) at GPACS

		Alkanes/ ppbv	Alkenes/ ppbv	Aromatics /ppbv	VOCs/ ppbv	NO <sub>x</sub> / ppbv	O <sub>3</sub> / ppbv
Spring	March	20.84	5.26	8.50	34.60	76.39	12.46
	April	25.11	5.86	11.33	42.30	35.17	16.02
	May	21.45	5.47	10.94	37.86	25.29	24.55
Summer	June	19.74	6.62	14.23	40.60	24.40	24.26
	July	20.07	6.72	12.90	39.69	24.70	24.26
	August	22.36	9.12	9.99	41.46	21.75	28.26
	September	20.82	7.80	8.95	37.57	25.18	29.67
Autumn	October	22.26	5.63	8.89	36.78	26.59	25.34
	November	39.16	10.24	14.16	63.57	39.98	21.78
	December	33.61	8.47	5.97	48.05	39.14	20.37
Winter	January	32.13	7.96	7.54	47.63	34.82	9.31
	February	-	-	-	-	52.69	9.97

**Table 4.** Photochemical properties of VOCs and their average mixing ratios at GPACS from June 2011 to May 2012.

Compound	MIR <sup>a</sup>	K <sup>b</sup> <sub>OH</sub> × 10 <sup>12</sup>	Mixing ratio (ppbv)	Mixing ratio (ppbc)
Alkanes				
Ethane	0.25	0.27	3.66	7.31
Propane	0.46	1.15	4.34	13.02
i-Butane	1.18	2.34	2.67	10.68
n-Butane	1.08	2.54	3.07	12.28
Cyclopentane	2.24	5.16	0.15	0.77
i-Pentane	1.36	3.9	1.72	8.61
n-Pentane	1.22	3.94	1.37	6.86
Methylcyclopentane	1.46	5.1	0.32	1.94
2,3-Dimethylbutane	1.07	6.3	0.13	0.76
2-Methylpentane	1.4	5.6	0.88	5.29
3-Methylpentane	1.69	5.7	0.75	4.51
n-Hexane	1.14	5.6	1.43	8.56
2,4-Dimethylpentane	1.11	5.7	0.37	0.41
Cyclohexane	1.14	7.49	1.65	9.90
2-Methylhexane	1.09	6.9	0.58	4.04
2,3-Dimethylpentane	1.25	5.1	0.26	1.82
3-Methylhexane	1.5	5.1	0.52	3.66
2,2,4-Trimethylpentane	1.2	3.68	0.22	1.79
n-Heptane	0.97	7.15	0.32	2.24
Methylcyclohexane	1.56	10.4	0.26	1.81
2,3,4-Trimethylpentane	0.97	7	0.12	0.96
2-Methylheptane	1.12	8.3	0.08	0.66
3-Methylheptane	0.8	8.6	0.08	0.68
n-Octane	0.68	8.68	0.19	1.54
n-Nonane	0.59	10.2	0.35	3.18
n-Decane	0.52	11.6	0.03	0.29
n-Undecane	0.47	13.2	0.17	1.92
n-Dodecane	0.38	14.2	0.14	1.65
Alkenes				
Ethene	7.4	8.5	2.99	5.97
Propene	11.57	26.3	1.32	3.96
trans-2-Butene	15.2	64	0.28	1.14
1-Butene	9.57	31.4	0.44	1.77
cis-2-Butene	14.26	56.4	0.22	0.86
trans-2-Pentene	10.47	67	0.03	0.15
1-Pentene	7.07	31.4	0.05	0.23
cis-2-Pentene	10.28	65	0.19	0.97
Isoprene	10.48	101	1.14	5.72
1-Hexene	—	—	0.67	3.99

Aromatics				
Toluene	3.93	5.96	4.59	32.10
Ethylbenzene	2.96	6.96	1.48	11.81
m,p-Xylene	8.54	20.5	1.41	11.24
Styrene	1.66	58	0.41	3.25
o-Xylene	7.58	13.6	0.66	5.28
i-Propylbenzene	2.45	6.6	0.10	0.86
n-Propylbenzene	1.96	5.7	0.23	2.05
m-Ethyltoluene	7.39	18.6	0.25	2.22
p-Ethyltoluene	4.39	11.8	0.21	1.89
1,3,5-Trimethylbenzene	11.75	56.7	0.21	1.86
o-Ethyltoluene	5.54	11.9	0.27	2.47
1,2,4-Trimethylbenzene	8.83	32.5	0.21	1.92
1,2,3-Trimethylbenzene	11.94	32.7	0.15	1.32
m-Diethylbenzene	7.08	15	0.12	1.25
p-Diethylbenzen	4.39	10	0.11	1.05

MIR<sup>a</sup> denotes maximum incremental reactivity (Carter, et al., 1994)

k<sub>OH</sub><sup>b</sup> denotes rate constant of VOCs react with hydroxyl radicals at 298K,(Atkinson and Arey,2003)

**Table 5.** Top 10 VOCs species at GPACS based on the Propy-Equiv and MIR scales from June 2011 to May 2012.

OH Reactivity Rank		MIR Rank	
Compound	Percentage (%)	Compound	Percentage (%)
Isoprene	19.97	Toluene	16.26
m,p-Xylene	7.97	m,p-Xylene	12.48
Toluene	6.62	Isoprene	7.99
Styrene	6.51	Propene	6.30
1,3,5-Trimethylbenzene	3.82	Ethene	6.07
Propene	3.60	o-Xylene	5.21
Ethylbenzene	2.85	Ethylbenzene	4.54
Cyclohexane	2.56	1,3,5-Trimethylbenzene	2.87
trans-2-Butene	2.51	trans-2-Butene	2.37
o-Xylene	2.48	1,2,4-Trimethylbenzene	2.22

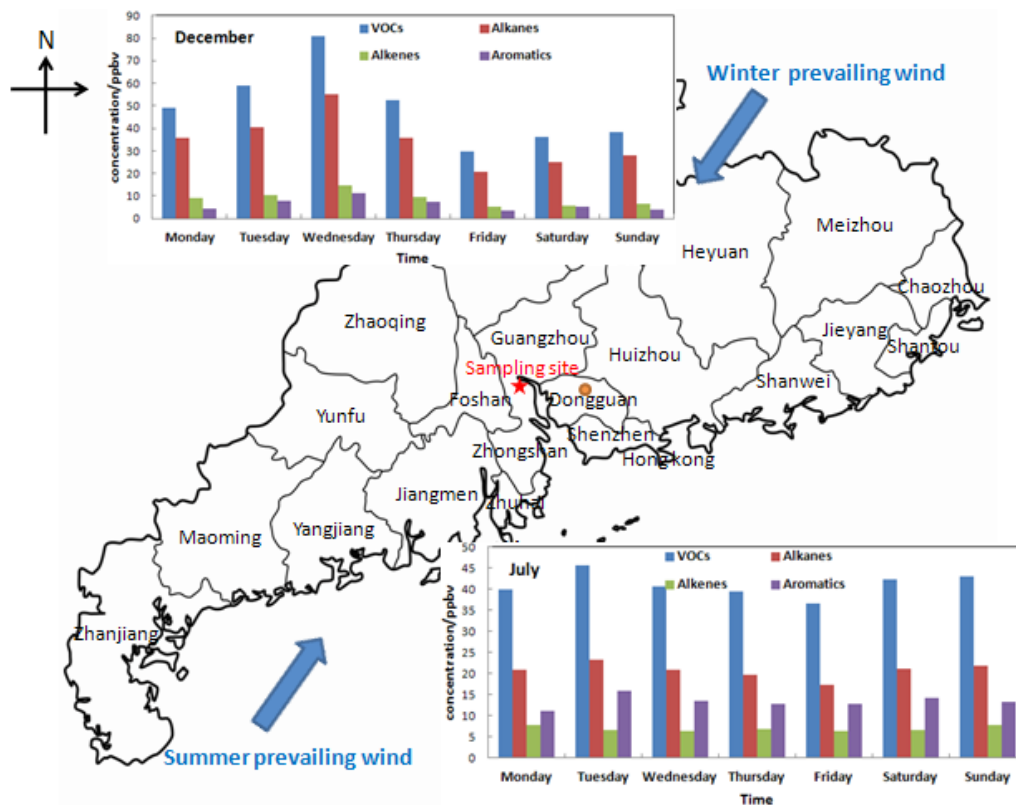


**Figure. 1.** The location of observation site at GPACS and its surrounding area, the pentagram represents the sampling site, and the circle represents the Dongguan City. The VOCs concentration in July when the summer prevailing wind is SW and in December when the winter prevailing wind is NE are showed in the map.

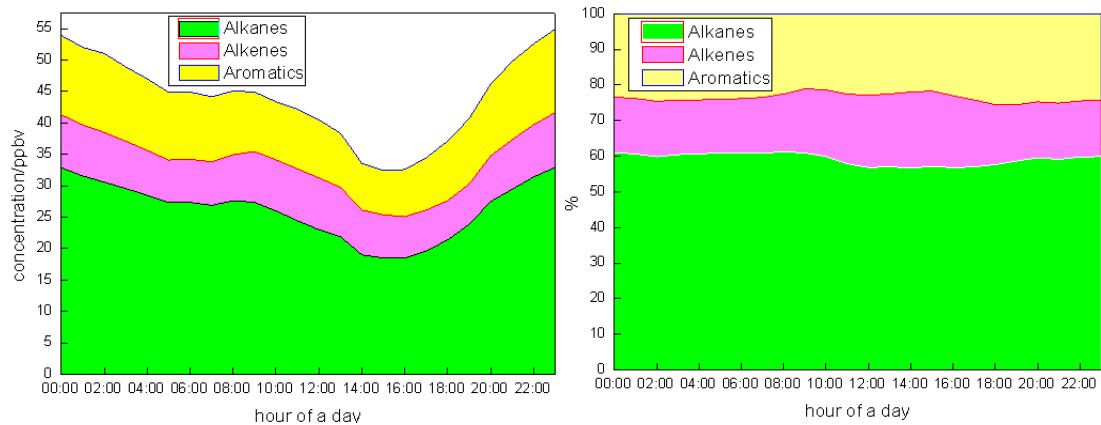


**Figure. 2.** Daily cycle of hourly averaged concentration of three categories of VOCs in ppbv and in % of total (from June 2011 to May 2012) at GPACS

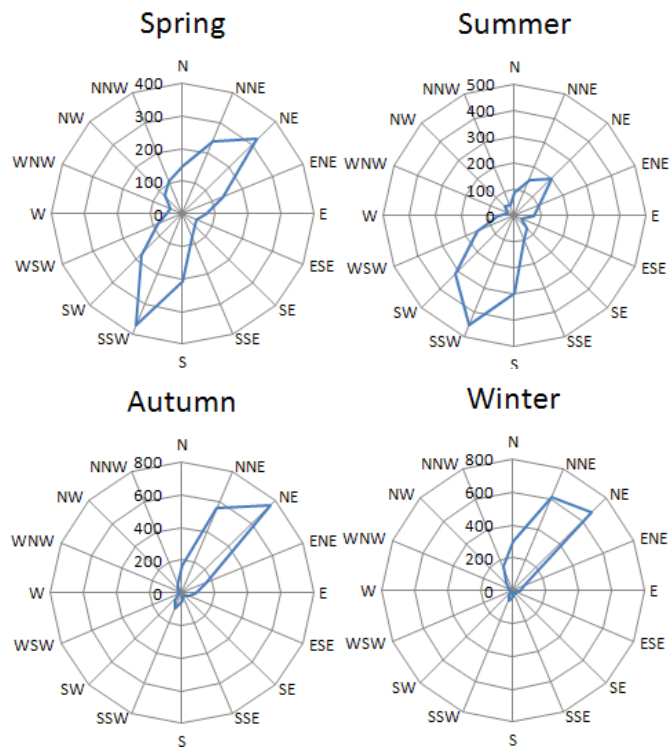


**Fig. 3.** The frequency of wind direction plotted by wind rose for four seasons (from June 2011 to May 2012) at GPACS

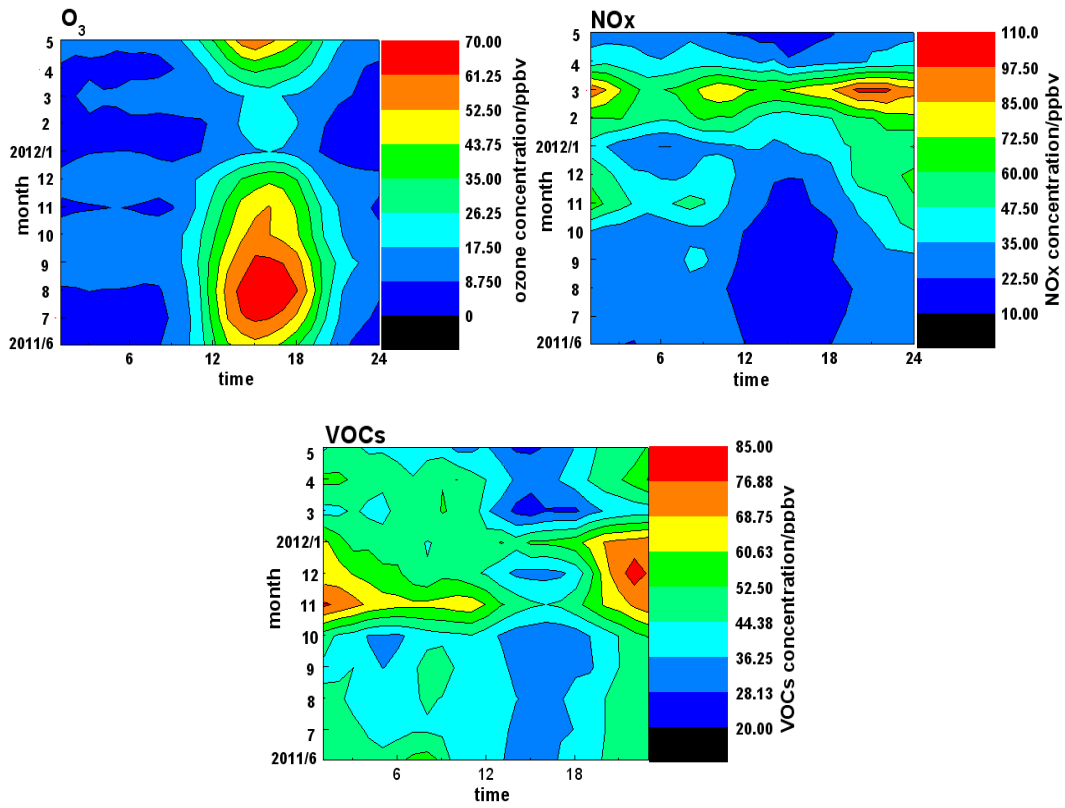


**Fig. 4.** The diurnal variations of ozone,  $NO_x$  and VOCs in months (from June 2011 to May 2012) at GPACS.



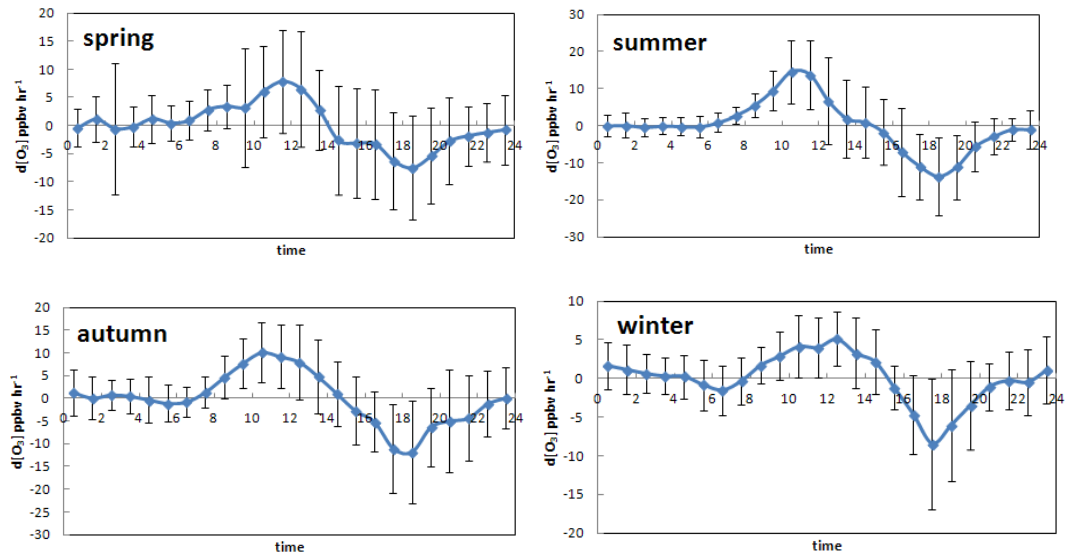


**Fig. 5.** Average diurnal trends in ozone from different seasons during June 2011 to May 2012 at GPACS. Colored marker represents hourly mean value. The black line gives the standard deviation.

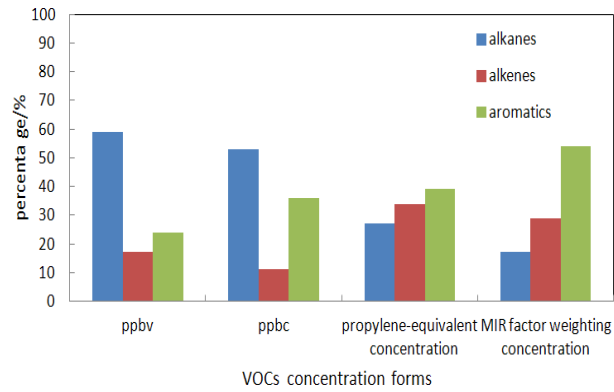


**Fig. 6.** Average fractions of each category based on volume mixing ratio (ppbv), carbon-atom-based concentration (ppbC), OH-reactivity-based Propy-Equiv concentration (ppbC), and MIR factor weighting concentration. Fractions of each VOCs category (alkanes, alkenes and aromatics) plotted by bar on four VOCs concentration form (ppbv, ppbc, propylene-equivalent concentration and MIR factor weighting concentration) from June 2011 to May 2012 at GPACS.

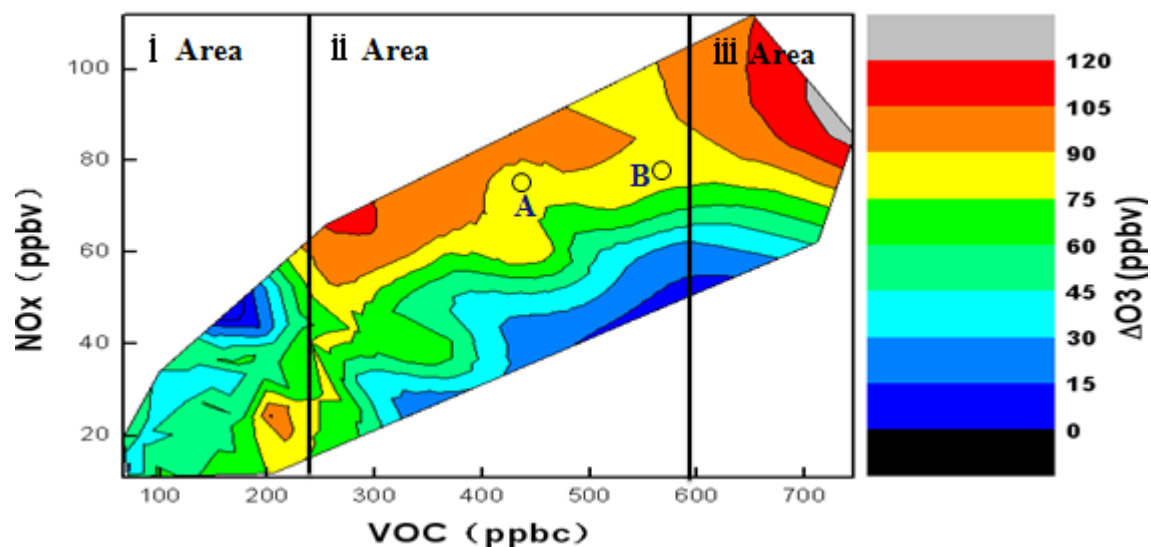


**Fig. 7.** The relationship among VOCs, NO<sub>x</sub> and the amount of O<sub>3</sub> increase ( $\Delta O_3$ ) was plotted by observational data from June 2011 to May 2012. The observational data are selected by the days when the sum of the solar radiation from sunrise to 18:00 exceeds the annual average and when the average wind speed from sunrise to 18:00  $< 3 \text{ms}^{-1}$ . The average concentrations of VOCs and NO<sub>x</sub> in the early morning (6:00-9:00) are used, and the amount of O<sub>3</sub> increase ( $\Delta O_3$ ) is defined as the difference between the maximum value in (10:00-18:00) and the average value in the early morning (6:00-9:00).

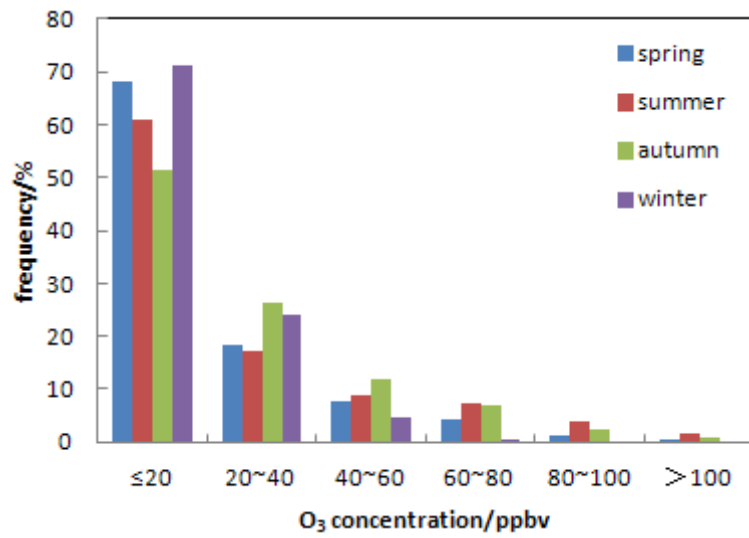


**Fig. 8.** The seasonal distribution frequency of hourly ozone concentration at GPACS, the frequency of hourly ozone concentration in each corresponding season is plotted by bar.

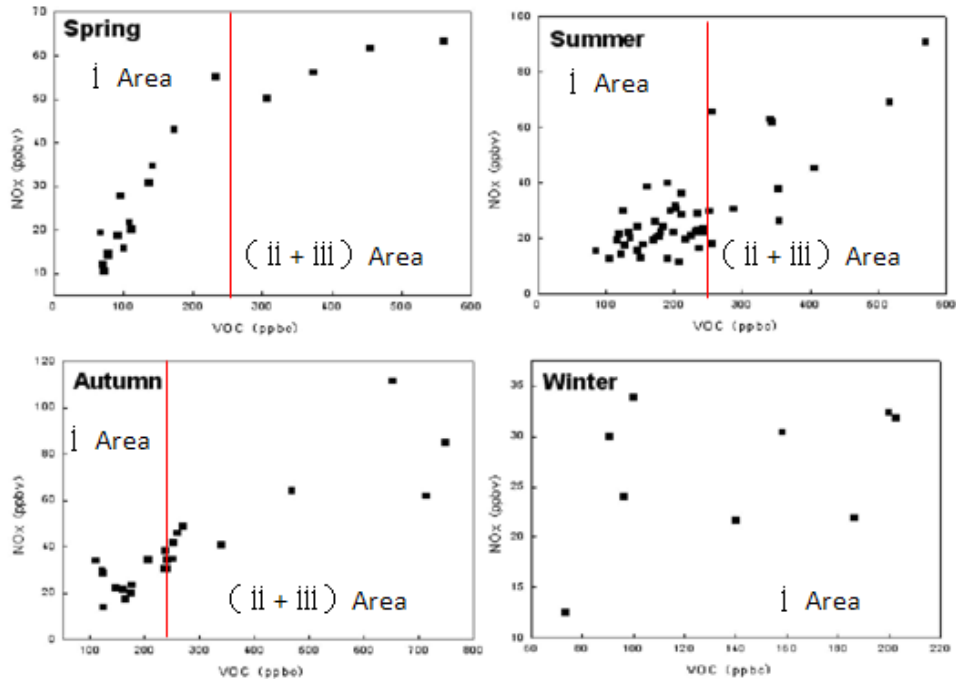


**Fig. 9.** The scatter diagram between VOCs and NOx by observational data from June 2011 to May 2012 selected by the days when the sum of the solar radiation from sunrise to 18:00 exceeds the annual average and when the average wind speed from sunrise to 18:00  $< 3\text{ms}^{-1}$ . i area and (ii+iii) area are divided by the red full line, i area denotes that the VOCs concentration below 250ppbc, (ii+iii) area denotes that the VOCs concentration above 250ppbc.

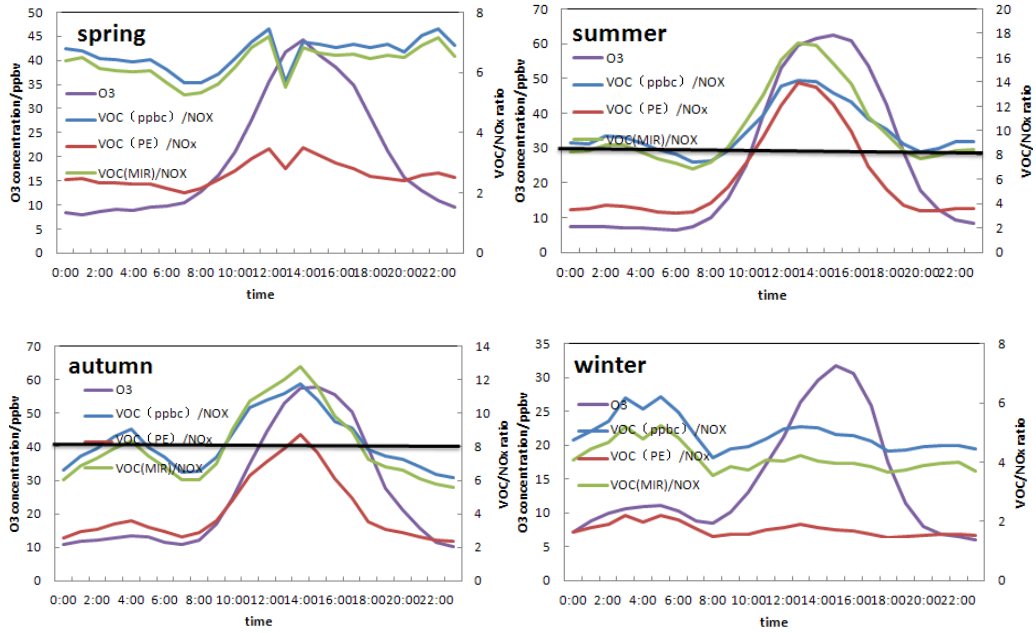


**Figure.10.** The variation patterns of VOC/NO<sub>x</sub> ratio and ozone concentration at four seasons (from June 2011 to May 2012) at GPACS. Three forms of VOC (ppbc, PE and MIR) is presented by blue, red and green respectively and colored markers represent hourly mean value. A black full line represents the VOC/NO<sub>x</sub>(8).

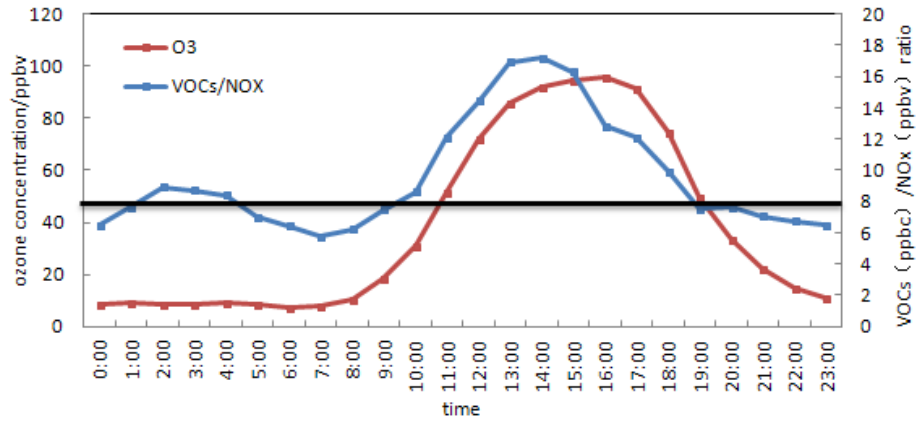


**Fig. 11.** The variation patterns of VOC/NO<sub>x</sub> ratio and ozone concentration at high ozone episode at GPACS. Colored markers represent hourly mean value. High ozone episode refers to the day with an hourly ozone value higher than 93ppbv. A black full line represents the VOC/NO<sub>x</sub>(8).